Product Identification and Kinetics of Reactions of HCl with $HNO_3/H_2SO_4/H_2O$ Solutions

Christopher D. Cappa, Sarah E. Kuipers, Jeanine M. Roberts, Abigail S. Gilbert, and Matthew J. Elrod*

Department of Chemistry, Hope College, Holland, Michigan 49423

Received: July 29, 1999; In Final Form: January 11, 2000

The gas-phase products of the reaction between $HNO_3/H_2SO_4/H_2O$ acid solutions and HCl were identified using IR and UV−Vis spectroscopy and chemical ionization mass spectrometry. The major products of the reaction were Cl_2 and ClNO, with quantifiable amounts of $ClNO_2$ sometimes present. On the basis of quantitative product yield determinations, the overall proposed reaction is $3HCl + HNO_3 \rightarrow Cl_2 + ClNO + 2H_2O$. Kinetic studies were also performed and the reaction was found to follow a second-order rate law: Rate $= k[HCl][HNO_3]$. On the basis of the products and intermediates observed and the rate law, a mechanism is proposed which involves the NO_2^+ ion as the key reactive species. The rate of the reaction is shown to depend strongly on the total acid concentration of the solution and temperature-dependent studies were also performed. The potential significance of this reaction in connection to stratospheric ozone depletion is evaluated by using the composition and temperature dependence of the rate to estimate the chlorine activation rate at polar stratospheric conditions.

Introduction

The importance of heterogeneous reactions involving $ClONO_2$, HCl, N_2O_5, and H_2O on polar stratospheric cloud (PSC) particles has been well established in connection with the observation of large-scale ozone depletion during the Antarctic springtime.[1,2] Laboratory studies have shown that both solid and liquid particles can promote heterogeneous reactions such as the following, converting the relatively inert chlorine reservoir molecules ($ClONO_2$ and HCl) into species (Cl_2 and HOCl) which are readily photolyzed to yield chlorine radicals:

$$ClONO_2 + H_2O \rightarrow HOCl + HNO_3 \quad (1)$$

$$HOCl + HCl \rightarrow Cl_2 + H_2O \quad (2)$$

$$ClONO_2 + HCl \rightarrow Cl_2 + HNO_3 \quad (3)$$

Although thermodynamic stability considerations indicate that PSCs should be composed of solid particles (either as nitric acid trihydrate or water ice) under winter Antarctic conditions,[3] an increasing preponderance of evidence suggests that PSCs may more often exist as supercooled liquid solutions of H_2SO_4, HNO_3, H_2O, and HCl.[4] In addition, although the atmospheric conditions necessary for efficient heterogeneous chlorine activation have been well established by laboratory[5] and field observation[6] data, there is little consensus concerning the detailed chemical mechanisms which give rise to the overall reactions given above. In particular, there is substantial debate concerning the role of surface vs bulk reactivity and whether the mechanisms proceed through covalent or ionic reactions.[7] Indeed, because of the early focus on solid PSC substrates, the potential roles of bulk phase reactions and ionic mechanisms have received relatively less scrutiny.

* To whom correspondence should be addressed (E-mail: elrod@hope.edu; telephone: (616) 395-7629; Fax: (616) 395-7118).

The predominant industrial processes for the production of Cl_2 rely on the catalytic oxidation of HCl as is the case for the heterogeneous reactions listed above (1−3).[8−10]

$$4HCl + O_2 \xrightarrow[\text{or}\ NOHSO_4\ \text{catalyst}]{HNO_3/H_2SO_4} 2Cl_2 + 2H_2O \quad (4)$$

The simplicity of this overall reaction is misleading, because a several stage reactor is required to efficiently regenerate the catalysts and to produce high yields. A more direct method to produce Cl_2 and ClNO directly from a reaction between HNO_3 and HCl[11] has also been reported:

$$3HCl + HNO_3 \rightarrow Cl_2 + ClNO + 2H_2O \quad (5)$$

Because these industrial chemistry processes are based on the chemical components present in PSCs and are potential chlorine activation pathways (because the chlorine-containing products of reactions 4 and 5 are readily photolyzed to chlorine radicals in the atmosphere), we have chosen to investigate the chemical reactivity of $HNO_3/H_2SO_4/H_2O/HCl$ solutions. Recently, there have been some reports of the reactivities of these solutions,[12,13] but a complete product study and a measurement of the rate of the reaction have not been performed. Therefore, we undertook a detailed study of the gas phase products of this reaction and temperature-dependent kinetics studies were performed to allow an extrapolation of the collected data to stratospherically relevant PSC compositions and temperatures in order to estimate the contribution of such reactions to chlorine activation.

Experimental Section

Product Studies—Flow-Through Method. The gas-phase products of the reaction between HCl and $HNO_3/H_2SO_4/H_2O$

10.1021/jp992666p CCC: $19.00
Published on Web 04/21/2000

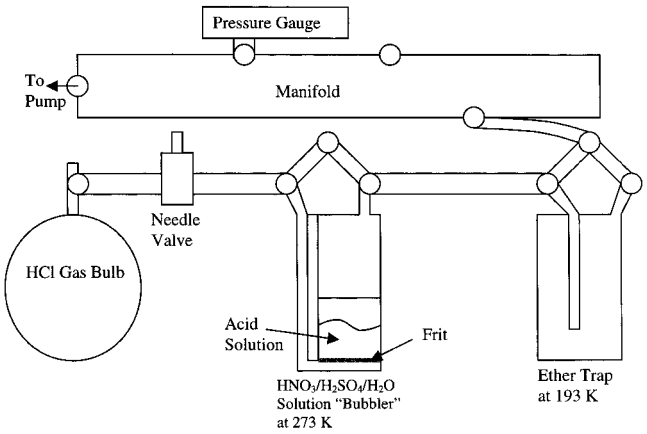

Figure 1. The closed system flow-through reactor.

solutions ranging from 45 to 95 wt % total acid were investigated using a closed system flow-through reactor (Figure 1). For each trial the gas bulb was filled with ~760 Torr HCl. The bubbler was loaded with 10 mL of a $HNO_3/H_2SO_4/H_2O$ solution. Bulk acid solutions used were prepared by diluting 70 wt % HNO_3 and 95 wt % H_2SO_4 with distilled water. The acid solution was maintained at 273 K using an ice bath. The system was evacuated (except for the HCl gas bulb) and then isolated. The evacuated pressure was a few Torr due to the vapor pressure of the acid solution. The pressure gradient between the gas bulb and the rest of the system was used to force the HCl to bubble through the nitric/sulfuric acid solution. The rate of gas flow through the acid solutions was controlled using a needle valve and set such that the slowest visible rate of bubbling through the solution was observed. As the reaction progressed, the valve was opened further to maintain the desired flow rate. Once the needle valve was completely open and no more bubbling was seen, the reaction was considered complete (usually 1−2 h), although some HCl remained in the gas bulb because of the finite pressure in the rest of the system. The products were trapped using an ethyl ether/liquid nitrogen cold trap at 193 K. Vapor pressure differences between the products and any unreacted HCl at this temperature allowed for preferential condensation of the products in the trap while leaving the unreacted HCl in the gas phase. This aided the analysis of the products and helped to drive the reaction by keeping the pressure relatively low on the collection side of the bubbler. When the reaction was completed and the products were condensed in the cold trap, the pressure of HCl remaining in the gas bulb was measured to determine the amount of HCl exposed to the acid solution. The system was evacuated and the products were allowed to warm and expand through the manifold system into an evacuated gas bulb. The total pressure of the gaseous products in the system was then measured.

A variety of other solutions in addition to the $HNO_3/H_2SO_4/H_2O$ solutions were also analyzed. $HONO/H_2SO_4/H_2O$ solutions were prepared by dissolving $NaNO_2$ in sulfuric acid solutions.[14] $NaNO_3/H_2SO_4/H_2O$ solutions were prepared by mixing $NaNO_3$ in 60 wt % H_2SO_4. For some trials, instead of using gaseous HCl, 1 g of NaCl was dissolved in various $HNO_3/H_2SO_4/H_2O$ solutions by freezing the acid, adding the salt, and letting the acid thaw. A 40% nitrosyl sulfuric acid ($NOHSO_4$, NSA) solution in H_2SO_4 was also used in place of the $HNO_3/H_2SO_4/H_2O$ solutions.

Product Identification. Some samples were diluted with N_2 and analyzed using a chemical ionization mass spectrometry (CIMS) apparatus described by Scholtens et al.[15] Unreacted HCl and the products Cl_2 and ClNO were detected according to the following reactions with SF_6^-:[16,17]

$$HCl + SF_6^- \rightarrow FHCl^- + SF_5 \quad (6)$$

$$Cl_2 + SF_6^- \rightarrow Cl_2^- + SF_6 \quad (7)$$

$$ClNO + SF_6^- \rightarrow Cl^- + NO + SF_6 \quad (8)$$

Unreacted HCl and the products ClNO, $ClNO_2$, and HONO were detected using FT-IR spectroscopy via the observation of characteristic vibrational bands at 2886, 1800, 651, and 856 cm^{-1}, respectively.[18]

Product Quantification. An IR gas cell with KBr windows and a UV−Vis gas cell with quartz windows were simultaneously filled with a sample of the collected product. The pressure of the product to be analyzed was recorded. An IR spectrum was recorded and the absorbance was measured at 1800 cm^{-1} where ClNO has a unique vibrational band (υ_1).[18]

To quantify the ClNO present, the molar absorptivity coefficient for ClNO was determined at 1800 cm^{-1} via the following procedure. Pure ClNO was prepared according to the method described by Longfellow et al.[14] Gaseous Cl_2 and NO were frozen together in their stoichiometric ratio (1:2). The mixture was warmed in an ice bath to allow the gases to react and then cooled to 195 K in an acetone/CO_2 bath. The mixture was pumped at this temperature until the pressure reached 5 Torr (the vapor pressure of ClNO at 195 K), indicating that the remaining sample was free of Cl_2 and NO. FT-IR and CIMS methods were used to confirm that only ClNO was present in the sample. The molar absorptivity coefficient for ClNO was determined at 1800 cm^{-1} from a 3.1 Torr sample of ClNO via Beer's Law to give the value $\sigma^{ClNO}_{1800\ cm^{-1}} = 0.0325\ cm^{-1}\ Torr^{-1}$. This value was used to determine the partial pressure of ClNO in the product samples:

$$P_{ClNO} = \frac{A_{1800\ cm^{-1}}}{\sigma^{ClNO}_{1800\ cm^{-1}} l} \quad (9)$$

where P is the partial pressure of ClNO in Torr, l is the path length (10 cm), and $A_{1800\ cm^{-1}}$ is the absorbance at 1800 cm^{-1}.

UV−Vis spectroscopy was used to measure the absorbance of the product samples at 330 and 260 nm. At 260 nm ClNO and $ClNO_2$ absorb much more strongly than Cl_2 (see Table 1 for relevant cross sections). If we assume that Cl_2 contributes negligibly to absorption at this wavelength, the partial pressure of $ClNO_2$ is determined by calculating the expected absorption due to ClNO (determined from eq 9 and Beer's Law) and taking the difference between the measured absorption and the calculated value for ClNO:

$$P_{ClNO_2} = \frac{A_{260\ nm} - P_{ClNO}\,\sigma^{ClNO}_{260\ nm} l}{\sigma^{ClNO}_{260\ nm} l} \quad (10)$$

TABLE 1: UV Cross Sections for ClNO, Cl_2, HONO, and $ClNO_2$

	σ^a (10^{-4} $torr^{-1}$ cm^{-1}) wavelength, nm	
molecule	260	330
$ClNO_2$	86.2	8.21
ClNO	24.6	20.7
Cl_2	0.281	35.8
HONO	−	15.6

[a] From ref 32.

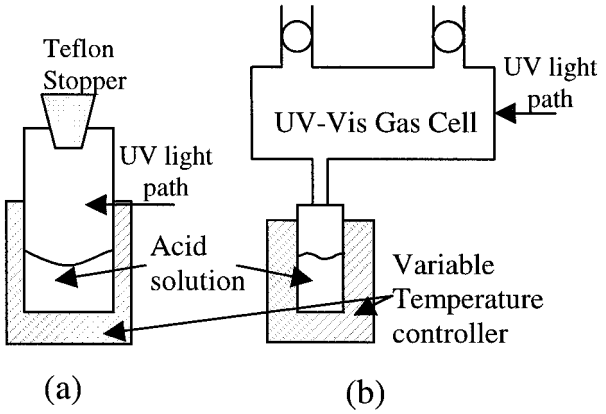

Figure 2. Kinetics configurations: (a) configuration 1; (b) configuration 2.

This was repeated using the measured absorption at 330 nm and subtracting the calculated values for ClNO and $ClNO_2$ (determined from eq 10) to determine the partial pressure of Cl_2:

$$P_{Cl_2} = \frac{A_{330\ nm} - P_{ClNO}\sigma_{330\ nm}^{ClNO} l - P_{ClNO_2}\sigma_{330\ nm}^{ClNO_2} l}{\sigma_{330\ nm}^{Cl_2} l} \quad (11)$$

The sum of the partial pressures was then calculated to allow a comparison to the measured pressure of gas sample analyzed:

$$P_{total} = P_{Cl_2} + P_{ClNO} + P_{ClNO_2} \quad (12)$$

The moles of products formed were calculated from the partial pressures, system volume, temperature, and the ideal gas law. The percent product yield was calculated as the moles of product per moles of exposed HCl × 100.

$$\%\ Cl_2\ yield = \frac{n_{Cl_2}}{n_{HCl\ used}} \times 100 \quad (13)$$

$$\%\ ClNO\ yield = \frac{n_{ClNO}}{n_{HCl\ used}} \times 100 \quad (14)$$

$$\%\ ClNO_2\ yield = \frac{n_{ClNO_2}}{n_{HCl\ used}} \times 100 \quad (15)$$

The total yield is the sum of the Cl_2, ClNO, and $ClNO_2$ yields.

Kinetic Studies. The production of gas-phase products from the reaction between the acid solutions and HCl was monitored over time at 330 nm using a UV−Vis spectrophotometer and two different product sampling configurations (Figure 2). For the studies performed with sampling configuration 1, the $HNO_3/H_2SO_4/H_2O$ solutions were precooled in a refrigerated bath to the desired temperature and the glass reaction container was precooled in the UV−Vis cell holder. A 10−75 μL sample of concentrated HCl was added to the reaction cell and then 1 mL of a $HNO_3/H_2SO_4/H_2O$ acid solution was added. A Teflon stopper was used to seal the cuvette during the reaction. As shown in Figure 2, the gas phase products were monitored by passing the beam path just above the solution. Kinetics runs for high total acid solutions at room temperature were typically obtained in ~10 min, whereas low total acid solutions at low temperatures were obtained in ~24 h. For the 50% HNO_3/50% H_2O solution kinetics trials, product sampling configuration 2 was used (see Figure 2). This design allows for the physical separation of the reaction solution and the detection of the gaseous products, which is desirable for the low-temperature measurements. For each kinetics run using this configuration, the same procedure as above was followed, however, once the HCl and acid solutions were mixed the kinetics apparatus was evacuated to ~5 Torr. Approximately 1 min of monitoring time was lost during this pump-down procedure. Despite the evacuation step, for most solutions the apparent reaction rate was in fact the diffusion rate of the gas-phase products from the liquid reactor to the gas-phase sampling cell. However, for the 50% HNO_3/50% H_2O solution, the reaction was slow enough such that this diffusion process did not affect the observed rate. This result was determined by measuring the rate of reaction for various solutions using both product sampling configurations. For all but the 50% HNO_3/50% H_2O solution the reaction rates were slower using configuration 2 than those using configuration 1, thus indicating that this diffusion process was indeed a problem for the other solutions. However, the use of the configuration 2 design was critical for accurately determining the rate of the 50% HNO_3/50% H_2O solutions for temperatures at or below 0 °C

Temperature Dependence of the Rate Constant. The temperature dependence of the rate constant was determined by measuring the reaction rate over a range of temperatures using UV−Vis spectroscopy monitoring at 330 nm. The study was limited by the decomposition of HNO_3 at temperatures greater than 30 °C and by the slowing of the reactions at low temperatures (−10 °C) so as to make the total time required to perform the kinetics experiment prohibitively long (>24 h). The refrigeration system was used to precool the acid solutions and the reaction container and to maintain a constant temperature throughout the reaction. For the 70% HNO_3/30% H_2O solution, product sampling configuration 1 was used and for the 50% HNO_3/50% H_2O solution product sampling configuration 2 was used.

Results and Discussion

Product Study. On the basis of the IR, UV−Vis, and CIMS data, Cl_2 and ClNO are the major gas phase products of the reaction of HCl with $HNO_3/H_2SO_4/H_2O$ solutions. Representative spectra are given in Figure 3. Quantifiable amounts of $ClNO_2$ were also sometimes observed and trace amounts of HONO were also sometimes detected. No other significant gas-phase species were identified. The relative yields for Cl_2, ClNO, and $ClNO_2$ were calculated for a variety of different solutions (Table 2) via eqs 13−15. Solutions A−H differ in total acidity as well as the relative amounts of HNO_3 or H_2SO_4. Comparison between the results for solution A and solutions B−H show that HNO_3 is necessary for the conversion of HCl into chlorine-containing products; i.e., H_2SO_4 does not react with HCl without HNO_3 present. However, the results for solution F show that HNO_3 can react with HCl in the absence of H_2SO_4. Comparison of the results between solutions C to D and F to G show that as the wt % HNO_3 is increased at a constant total acid wt %, the efficiency of the reaction increases dramatically. At a constant wt % HNO_3 the yield increases as the total acidity increases, as evidenced by the results for solutions B, D, and G. The total yields ranged anywhere from 0 to nearly 100%, depending on the composition of the solution. As will be discussed later, the observed yield differences are due to a kinetic effect, not a thermodynamic effect. Thus, these results do not represent the equilibrium distribution of species. To ensure that the majority of the products had been identified the observed pressure was compared to P_{total} from eq 12. The two values were found to

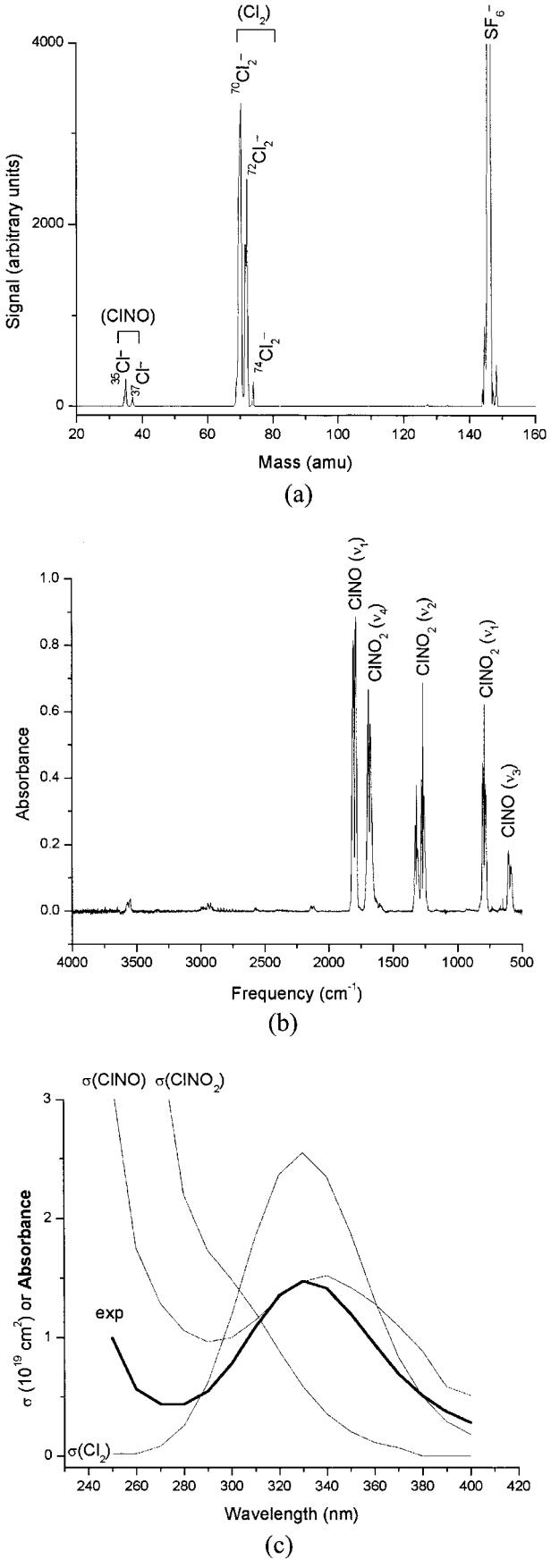

Figure 3. Representative (a) CIMS, (b) IR, and (c) UV−Vis (with relevant cross sections for Cl_2, ClNO, and $ClNO_2$ overlaid) spectra. Note that the sensitivity of each technique to each product is different, and therefore simple comparisons of peak intensity are not indicative of the true product ratios.

agree within 20%, thus suggesting that no major products were overlooked.

The amount of $ClNO_2$ detected was widely variable, with it sometimes not detected as a product at all. Thus, we concluded that $ClNO_2$ is an intermediate in the reaction and the amount present depended on the varying approach to equilibrium for each experiment. On the other hand, Cl_2 and ClNO were always observed as major products and found to be present in about a 1:1 ratio, suggesting that these species are final products with a 1:1 stoichiometric ratio. On occasion, HONO was detected as a minor product. On the basis of the reactants and the observed gas-phase products, we propose the following overall reaction:

$$3HCl + HNO_3 \rightarrow Cl_2 + ClNO + 2H_2O \qquad (16)$$

Reaction 16 is the same reaction as is believed to occur in aqua regia.[19] We further suggest the following overall mechanism based on the observation of $ClNO_2$ and HONO as intermediates:

$$HCl + HNO_3 \rightarrow ClNO_2 + H_2O \qquad (17)$$

$$HCl + ClNO_2 \rightarrow Cl_2 + HONO \qquad (18)$$

$$HCl + HONO \rightarrow ClNO + H_2O \qquad (19)$$

$$3HCl + HNO_3 \rightarrow Cl_2 + ClNO + 2H_2O \qquad (16)$$

Recently, product studies have been reported on similar $HNO_3/H_2SO_4/H_2O/HCl$ systems. Luick et al. identified ClNO and $ClNO_2$ as products using FT-IR techniques,[12] whereas Massucci et al. identified Cl_2 using electron impact mass spectrometry,[13] in agreement with our IR/UV−Vis/CIMS results.

The most striking result from our product study is the dependence of the reaction yield on the total acid composition. Burley and Johnston investigated the identity of key nitrogen oxide species in sulfuric acid solutions. They found that NO_3^- was the predominant species for dilute acid solutions, NO_2^+ was the predominant species in very concentrated acid solutions, and HNO_3 was the predominant species for solutions of intermediate composition.[20] There are a number of potential ways that nitric acid could ionize to produce NO_2^+. The first of these involves direct dissociation of nitric acid to yield the reaction $HNO_3 \rightarrow NO_2^+ + OH^-$, however this reaction seems unlikely. A second process involves reaction between nitric acid and sulfuric acid to yield NO_2^+ as one of several ionic products: $HNO_3 + 2\,H_2SO_4 \rightarrow H_3O^+ + 2\,HSO_4^- + NO_2^+$. A third possibility is the reaction $2\,HNO_3 \rightarrow H_2O + NO_2^+ + NO_3^-$. This reaction is driven to the right by sulfuric acid which acts like a strong desiccant for the water product. Because we have shown that high reactivity is present in the absence of H_2SO_4, we propose that this ionization process is most likely responsible for the formation of NO_2^+ in our solutions. It has also been relatively well-established that Cl^- is the dominant species present when HCl is dissolved in acid solutions, although it may also be present as the solvated species $H_3O^+(H_2O)_nCl^-$.[21,22] That Cl^- is the reactive species in our experiments is supported by the results from solution K, where NaCl was used in place of HCl and chlorine containing products were still produced from the reaction. We therefore propose that the first step (eq 17) of the proposed mechanism is better represented as the following ionic process.

TABLE 2: Product Yields for Various Acid Solutions

solution	HNO_3 (wt %)	H_2SO_4 (wt %)	H_2O (wt %)	total acid (wt %)	ClNO (% yield)	Cl_2 (% yield)	$ClNO_2$ (% yield)	total (% yield)
A	0	95	5	95	0	0	0	0
B	1	94	5	95	2.9	3.7	0.9	7.5
C	25	60	15	85	20.2	27.9	6.9	55.0
D	1	84	15	85	0.9	1.2	0.4	2.5
E	45	35	20	80	32.6	44.4	9.8	86.9
F	70	0	30	70	20.9	19.0	0.5	40.4
G	1	69	30	70	1.0	1.0	0	1.9
H	40	5	55	45	0.9	0.4	0	1.3
I		0.4 M HONO in 79 wt % H_2SO_4			1.7	0	0	1.7
J		1 M $NaNO_3$ in 60 wt % H_2SO_4			1.1	0.9	0.7	2.7
K[a]	70	0	30		6.4	8.3	3.2	17.9
L		40% $NOHSO_4$ in H_2SO_4			26.5	0	0	26.5

[a] One gram of NaCl used in place of HCl.

$$2\,HNO_3 \rightarrow H_2O + NO_2^+ + NO_3^- \quad (20)$$

$$HCl \rightarrow H^+ + Cl^- \quad (21)$$

$$H^+ + NO_3^- \rightarrow HNO_3 \quad (22)$$

$$Cl^- + NO_2^+ \rightarrow ClNO_2 \quad (23)$$

$$HNO_3 + HCl \rightarrow H_2O + ClNO_2 \quad (17)$$

Thus, we surmise that the concentration of NO_2^+ (which is determined by both the HNO_3 concentration and the total acid concentration) directly influences the efficiency of the mechanism. Luick et al. proposed a reaction between NO_3^-, Cl^-, and H^+ in the formation of $ClNO_2$.[12] However, it seems unlikely that the efficiency of a mechanism involving these acid species would show such a strong total acid dependence.

We further propose that the second step of the mechanism (equation 18) is better written as a combination of three ionic reactions:

$$HCl \rightarrow H^+ + Cl^- \quad (21)$$

$$Cl^- + ClNO_2 \rightarrow Cl_2 + NO_2^- \quad (24)$$

$$NO_2^- + H^+ \rightarrow HONO \quad (25)$$

$$ClNO_2 + HCl \rightarrow Cl_2 + HONO \quad (18)$$

The conversion of NO_2^- to HONO is expected to be very efficient in the highly acidic solutions tested here. The third step (equation 19) may be better represented by the following ionic reactions:

$$HCl \rightarrow H^+ + Cl^- \quad (21)$$

$$Cl^- + HONO \rightarrow ClNO + OH^- \quad (26)$$

$$H^+ + OH^- \rightarrow H_2O \quad (27)$$

$$HCl + HONO \rightarrow ClNO + H_2O \quad (19)$$

However, HONO may not be the key species because in dilute sulfuric acid solutions HONO is most likely present as the hydrated nitrosonium ion (H_2ONO^+) and in concentrated solutions as nitrosyl sulfuric acid.[23,24] Therefore, eq 26 above could be replaced by either of the following reactions:

$$Cl^- + H_2ONO^+ \rightarrow ClNO + H_2O \quad (28)$$

$$Cl^- + NOHSO_4 \rightarrow ClNO + HSO_4^- \quad (29)$$

Our product studies performed on a solution of HONO, H_2SO_4, and HCl (solution I, Table 1) show that ClNO is the only chlorine-containing product. Our product studies on solutions of $NOHSO_4$, H_2SO_4, and HCl (solution L, Table 1) also show ClNO as the only chlorine-containing product. Therefore, on the basis of our results, we cannot rule out any of the above ionic reactions, so we arbitrarily choose reaction 26 in our ionic mechanism for reaction 19. We present an overall ionic mechanism to explain the overall reaction:

$$2\,HNO_3 \rightarrow H_2O + NO_2^+ + NO_3^- \quad (20)$$

$$3\,(HCl \rightarrow H^+ + Cl^-) \quad (21)$$

$$H^+ + NO_3^- \rightarrow HNO_3 \quad (22)$$

$$Cl^- + NO_2^+ \rightarrow ClNO_2 \quad (23)$$

$$Cl^- + ClNO_2 \rightarrow Cl_2 + NO_2^- \quad (24)$$

$$NO_2^- + H^+ \rightarrow HONO \quad (25)$$

$$Cl^- + HONO \rightarrow ClNO + OH^- \quad (26)$$

$$H^+ + OH^- \rightarrow H_2O \quad (27)$$

$$3\,HCl + HNO_3 \rightarrow Cl_2 + ClNO + 2H_2O \quad (16)$$

Kinetic Measurements. The gas phase products were monitored at 330 nm, and the cross sections are given in Table 1. Absorption at 330 nm is due mainly to Cl_2, ClNO, and HONO, with minimal contribution from $ClNO_2$, due to the small relative cross section. However, for solutions with a high total acidity the solubility of HONO is high, so it is assumed that HONO will contribute little to the measured absorption.[14,24,25] Therefore, monitoring the absorbance at 330 nm is a measure of the time dependence of the appearance of both products, Cl_2 and ClNO.

As a starting point, we assume that the rate law depends only on [HCl] and [HNO_3]. The measurements were made using a pseudo first-order kinetics situation ([HNO_3] $\gg$ [HCl]). Therefore, the assumed rate law is

$$\frac{d[\text{products}]}{dt} = k'[HCl] \quad (30)$$

and the integrated first-order rate law is

$$[\text{products}]_t = [HCl]_0 \times (1 - e^{-k't}) + C \quad (31)$$

where k' is the pseudo first-order rate constant and C is a

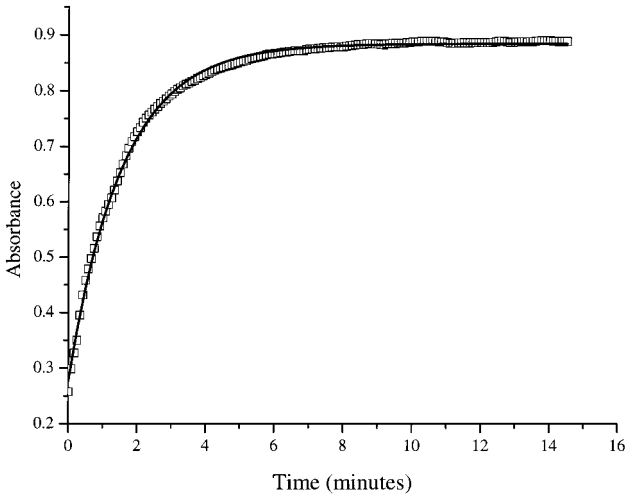

Figure 4. Typical kinetics data for an 80% total acid (40% HNO_3/40% H_2SO_4) solution at 298 K. The data were fit to eq 33.

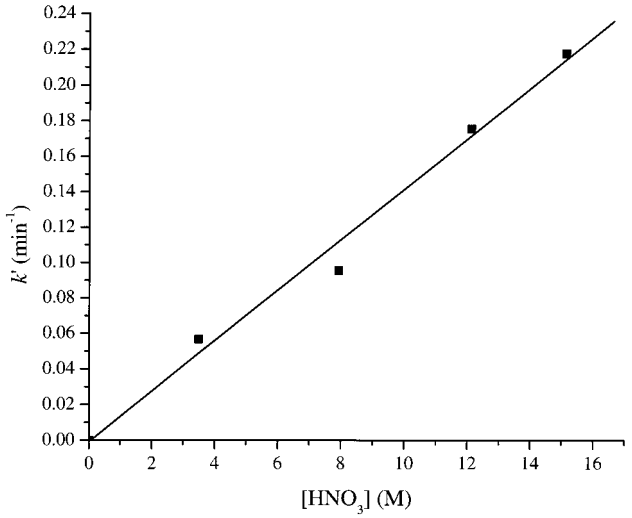

Figure 5. Plot of k' vs $[HNO_3]$ for 70% total acid at 298 K. Linear regression results: slope = $(1.44 \pm 0.15) \times 10^{-2}$ M^{-1} min^{-1}, intercept = $(-0.2 \pm 1.6) \times 10^{-2}$ min^{-1}.

constant of integration. As can be seen in Figure 4, the data can be fit according to the first-order integrated rate law very accurately ($\sigma_{k'}/k' = 0.0070$). The data were also fit according to a second order integrated rate law

$$[\text{products}]_t = -\frac{1}{\frac{1}{[\text{HCl}]_0} + k't} + [\text{HCl}]_0 \qquad (32)$$

However, this data analysis method led to a larger value of $\sigma_{k'}/k'$ (0.036) than for the first-order data analysis method. Therefore, the reaction is most likely first order in HCl. When k' is plotted against $[HNO_3]$, while maintaining a constant total acid concentration, a linear relationship is observed, indicating that the reaction is also first order in nitric acid (Figure 5). The overall phenomenological rate law for this reaction can therefore be written as

$$\frac{\text{d}[\text{products}]}{\text{d}t} = k_{16}[\text{HCl}][\text{HNO}_3] \qquad (33)$$

where the slope of a plot of k' vs $[HNO_3]$ yields the bimolecular rate constant k_{16} for the overall reaction. This suggests that our original assumption that the rate depends only on [HCl] and $[HNO_3]$ is valid. Further, this result indicates that the rate-limiting step is the first step (eq 17) in the proposed mechanism. We again wish to emphasize that we were unable to individually monitor the products and we have therefore measured an overall rate for the reaction by monitoring all of the products simultaneously. However, if the first step is indeed rate limiting, then monitoring products from that step and each subsequent step will give the same rate as if each product were monitored individually. For most trials the bimolecular rate constant was actually calculated from a single measurement of k' and $[HNO_3]$. $[HNO_3]$ was determined for each solution from the weight percent of nitric acid and the density of the solution. The density for each solution at all temperatures was estimated as a weighted average of the HNO_3, H_2SO_4, and H_2O densities at 25 °C. This approximation leads to densities that are too low, due to the nonideality of these strongly hydrogen-bonding systems. In addition, densities generally increase with decreasing temperature. Therefore, we estimate that our density calculations may deviate from the actual value by being up to 25% too low, leading to values for $[HNO_3]$ that are too low and bimolecular rate constants that are too high.

Table 3 gives the average bimolecular rate constant for various solutions of differing $[HNO_3]$ and total acid concentrations based on at least three individual kinetics trials. The dominant observed effect is the increase in the rate constant with increasing total acid content. Although we have determined that the phenomenological rate law is first order in both HCl and HNO_3, our product study results suggest the following rate law based on the role of ionic species:

$$\frac{\text{d}[\text{products}]}{\text{d}t} = k_{23}^{\text{ionic}}[\text{Cl}^-][\text{NO}_2^+] \qquad (34)$$

As discussed earlier, there is probably an exact correspondence between [HCl] and $[Cl^-]$ in our solutions. However, we propose that total acid dependence of k_{16} is because the rate law depends directly on $[NO_2^+]$ and indirectly on $[HNO_3]$. If we assume that the NO_2^+ concentration is proportional to the $[HNO_3]$ concentration for a given total acid concentration, our phenomenological rate law (which is first order in $[HNO_3]$) would be consistent with the rate law given in eq 34. Furthermore, if we assume that the $[NO_2^+]/[HNO_3]$ ratio depends on the activity coefficient of NO_2^+ (which will increase as the total acid concentration increases), we would predict that the phenomenological rate constant k_{16} should increase with total acid concentration, as is observed. Thus, it should be possible to parametrize our rate constant k_{16} in terms of the activity coefficient of NO_2^+ ($\gamma_{NO_2^+}$). However, we are not aware of a method to allow the calculation of $\gamma_{NO_2^+}$ for all of the solutions under study. A sophisticated model which does allow for the calculation of γ_{H_2O} has been reported by Carslaw et al.[26] Because the activity coefficients of NO_2^+ and H_2O should be inversely related, we attempted to parametrize our data in terms of γ_{H_2O}. The water activity coefficient γ_{H_2O} for each of the solutions was calculated at 273 K using the Carslaw et al. model and is given in Table 3. To parametrize the bimolecular rate constant in terms of an acid solution parameter, a plot of log k_{16} vs log γ_{H_2O} was found to be linear (Figure 6). The data were fit according to the equation $\log(k_{16}) = -0.87 \log(\gamma_{H_2O}) - 4.61$. This parametrization shows that k_{16} increases steeply as the total acidity increases. For example, at 25 °C for an 85 wt % total acid solution, $k_{16} = 1.40 \times 10^{-2}$ M^{-1} s^{-1}, while for a 50 wt % total acid solution, $k_{16} = 6.13 \times 10^{-5}$ $M^{-1}s^{-1}$. Therefore, a decrease in the total acid content from 85 to 50 wt % effects a decrease in the rate constant by a factor greater than 200.

TABLE 3: Kinetic Data and Water Activity Coefficients for Various Acid Solutions

T (K)	HNO_3 (wt %)	H_2SO_4 (wt %)	H_2O (wt %)	total acid (wt %)	k' (min^{-1})	[HNO_3] (M)	k_{16} (M^{-1} s^{-1})	γ_{H_2O}
298	5	80	15	85	1.11	1.32	1.40×10^{-2}	0.001
298	4	81	15	85	0.251	1.059	3.95×10^{-3}	0.001
298	2.5	82.5	15	85	0.503	0.663	1.26×10^{-2}	0.001
298	1.75	83.25	15	85	0.254	0.465	9.11×10^{-3}	0.001
298	1	84	15	85	0.631	0.266	3.95×10^{-2}	0.001
298	40	40	20	80	0.370	9.64	6.99×10^{-4}	0.023
298	35	45	20	80	0.200	8.50	3.91×10^{-4}	0.020
298	30	50	20	80	0.268	7.34	6.08×10^{-4}	0.017
298	25	55	20	80	0.442	6.16	1.20×10^{-3}	0.014
298	20	60	20	80	0.302	4.97	1.01×10^{-3}	0.012
298	70	0	30	70	0.218	15.1	2.79×10^{-4}	0.144
303	70	0	30	70	0.283	15.1	3.13×10^{-4}	0.144
288	70	0	30	70	0.0924	15.1	1.02×10^{-4}	0.144
283	70	0	30	70	0.0568	15.1	6.27×10^{-5}	0.144
273	70	0	30	70	0.0316	15.1	3.49×10^{-4}	0.144
298	55	15	30	70	0.175	12.1	2.41×10^{-4}	0.124
298	35	35	30	70	0.0954	7.92	2.01×10^{-4}	0.091
298	15	55	30	70	0.0567	3.49	2.71×10^{-4}	0.061
298	60	0	40	60	0.0382	12.3	5.17×10^{-5}	0.271
298	50	0	50	50	0.0324	9.79	6.13×10^{-5}	0.421
283	50	0	50	50	0.0152	9.79	2.58×10^{-5}	0.421
280.5	50	0	50	50	0.0130	9.79	2.21×10^{-5}	0.421
273	50	0	50	50	0.00722	9.79	3.40×10^{-5}	0.421
263	50	0	50	50	0.00356	9.79	6.07×10^{-6}	0.421

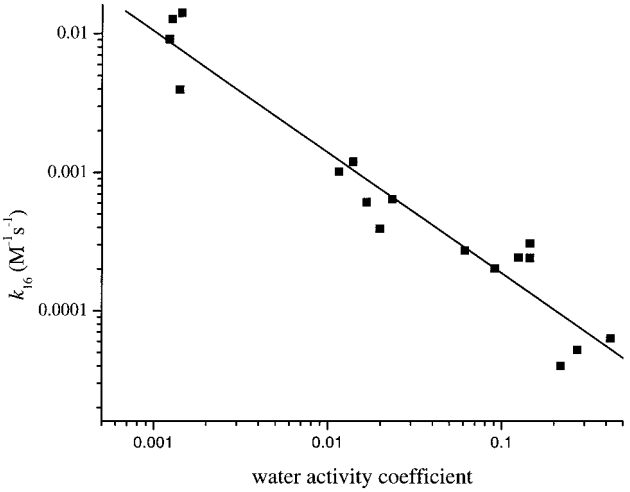

Figure 6. Double logarithmic plot of k_{16} vs γ_{H_2O}. Linear regression results: slope = -0.873 ± 0.062, intercept = -4.61 ± 0.11.

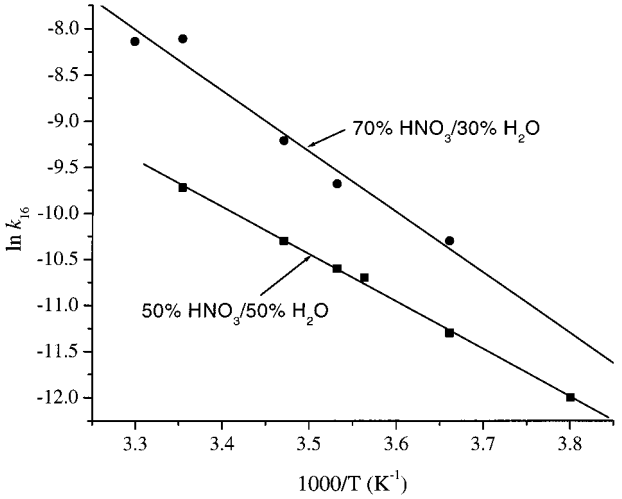

Figure 7. Arrhenius plot for the 50%/0%/50% (linear regression results: slope = -5170 ± 170 K, intercept = 7.66 ± 0.62) and 70%/0%/30% (linear regression results: slope = -6560 ± 690 K, intercept = 13.6 ± 2.4) $HNO_3/H_2SO_4/H_2O$ solutions.

Temperature Dependence of the Rate Constant. The dependence of the bimolecular rate constant on temperature was tested for both a 50%/0%/50% and a 70%/0%/30% solution ($HNO_3/H_2SO_4/H_2O$). As expected, the rate of reaction for these solutions decreases with temperature (as can be seen in Table 3). An Arrhenius plot (Figure 7) was made for each acid solution and the activation energy, E_a, of each reaction was determined. E_a for the 50%/0%/50% solution was 43.0 ± 2.8 kJ mol^{-1} and for 70%/0%/30% E_a was 54.6 ± 11.6 kJ mol^{-1} at the two standard deviation limit. It should be noted that the activation energies for the two solutions are statistically indistinguishable.

Atmospheric Implications—Chlorine Activation Rate Under Polar Stratospheric Conditions. Under typical stratospheric conditions (100 mbar, 16 km altitude, ~215 K) stratospheric aerosols are composed almost entirely of H_2SO_4 and water. However, during the Antarctic winter the temperature of the stratosphere can drop to less than 190 K, causing a drastic change in the composition of these aerosols. The thermodynamic model developed by Tabazadeh et al. predicts that for normal stratospheric conditions (100 mbar, $[HNO_3]_{gas} = 10.0$ ppbv, $[H_2O]_{gas} = 5.0$ ppmv, $[HCl]_{gas} = 2.0$ ppbv, $[H_2SO_4]_{aerosol} = 0.036\ \mu g \cdot m^{-3}$), the condensation point for HNO_3/H_2O solutions is about 195 K.[27] As this point is reached, uptake of HNO_3 is rapid and HNO_3 reaches a maximum concentration (~46 wt %) at 194 K. Accordingly, as the concentration of HNO_3 increases, the concentration of H_2SO_4 rapidly decreases to <2 wt % at 194 K. Similarly, the Henry's law coefficient for HCl drastically increases as temperature decreases from 215 to 194 K.[27] Therefore, as a first approximation, the rate of reaction 16 in polar stratospheric aerosols is constrained by the low temperatures required for significant concentrations of HNO_3 and HCl to be formed and by the decreasing rate constant as the temperature decreases.

To estimate the potential contribution of reaction 16 to chlorine activation under winter Antarctic conditions, we modeled PSCs as a supercooled liquid aerosol with a composition of 50% HNO_3/50% H_2O. We assume that the uptake of HNO_3 and HCl by the aerosols is fast relative to the rate of reaction 16, and simply use the thermodynamic equilibrium concentrations of HNO_3 and HCl in order to estimate the rate

of chlorine activation. The data from the Arrhenius plot for our results of this solution were extrapolated to the temperature corresponding to maximum HNO_3 concentration as predicted by the Tabazadeh et al. model (194 K). The rate constant at 194 K was calculated to be $5.7^{+12.3}_{-5.7} \times 10^{-9}$ M^{-1} s^{-1} at the two standard deviation limit. The HCl processing rate, which is a measure of chlorine activation for this reaction, was calculated from eq 35:

$$-\frac{d[HCl]_{gas}}{dt} = -\frac{d[HCl]_{aerosol}V_{aerosol}}{dt}\frac{}{V_{gas}} = 3 \times k_{16}[HCl]_{aerosol}[HNO_3]_{aerosol}\frac{V_{aerosol}}{V_{gas}} \quad (35)$$

where k_{16} is our extrapolated value, $[HNO_3]_{aerosol} = 9.3$ M and $[HCl]_{aerosol} = 0.13$ M are taken from the model used by Tabazadeh et al. assuming the conditions described above,[27] and $V_{aerosol}/V_{gas} = 2 \times 10^{-12}$ is the ratio between the volume of aerosols in the atmosphere to the total volume of gas in the atmosphere during the Antarctic winter.[28] The factor of 3 arises from the fact that 3 HCl molecules are processed for each complete cycle as required by the overall reaction stoichiometry. Using these parameters, we calculate a processing rate of ~24 molecules cm^{-3} s^{-1} for reaction 16. To assess the significance of this processing rate, the processing rate via reaction 16 was compared to the HCl processing rate for the reaction of $ClONO_2$ with HCl (reaction 3), the predominant chlorine activation route. To calculate the HCl processing rate for this heterogeneous reaction the temperature, composition of the aerosols, total aerosol surface area, $[ClONO_2]_{gas}$, and the reaction probability (which is dependent on temperature and composition) for the reaction must be known. Using the 194 K, 100 mbar total pressure conditions we used to estimate the HCl processing rate via reaction 16, the HCl processing rate via reaction 3 was calculated from eq 36:[14]

$$\frac{-d[ClONO_2]_{gas}}{dt} = \frac{-d[HCl]_{gas}}{dt} = \frac{\gamma \sigma_A c_{ClNO_2}[ClONO_2]_{gas}}{4} \quad (36)$$

where a lower limit for γ is estimated to be 0.25,[29] $\sigma_A = 1 \times 10^{-7}$ cm^{-1} is the aerosol surface area per unit volume,[30] c_{ClONO_2} is the mean thermal speed (223 m s^{-1}at 194 K), and $[ClONO_2]_{gas} = 6.8 \times 10^8$ molecules cm^{-3} is the gas-phase concentration of $ClONO_2$ in the stratosphere.[30] We calculate the HCl processing rate via the $ClONO_2$ + HCl heterogeneous reaction to be ~95,000 molecules cm^{-3} s^{-1}. Comparison of this value to our estimate of the HCl processing rate via reaction 16 (24 molecules cm^{-3} s^{-1}) shows that chlorine activation from reaction 16 is at most a minor chlorine activation pathway in comparison to the $ClONO_2$ + HCl heterogeneous pathway. Even if we consider the statistical upper limit for our value of k_{16} at 194 K (18.0×10^{-9} M^{-1} s^{-1}) we estimate a processing rate of only 79 molecules cm^{-3} s^{-1}, which is still minor in comparison. The processing rate via reaction 16 can also be compared to the major gas-phase chlorine activation pathway:

$$OH + HCl \rightarrow Cl + H_2O \quad (37)$$

We calculated the processing rate for reaction 37 from the following data: $k_{37}(194\ K) = 5.3 \times 10^{-13}$ cm^3 $molecules^{-1}$ s^{-1},[31] $[OH]_{gas} = 1 \times 10^6$ molecules cm^{-3},[32] and $[HCl]_{gas} = 5.0 \times 10^9$ molecules cm^{-3}.[32] Using these values the processing rate via reaction 37 is 2650 molecules cm^{-3} s^{-1}. Therefore, chlorine activation via reaction 16 can also be considered minor in comparison to the major gas-phase chlorine activation pathway.

Atmospheric Implications—Connection to Proposed Heterogeneous Mechanisms. In the heterogeneous reaction between HCl and $ClONO_2$, Cl^- from solvation of HCl is thought to react by nucleophillic attack on the partially electropositive Cl atom in $ClONO_2$.[33,34] To investigate whether a similar reaction in our proposed mechanism, Cl^- + $ClNO_2$, might proceed via a similar route, we sought to compare partial charge character of the chlorine atom on $ClNO_2$ to that for $ClONO_2$. Using electronic structure calculations,[35] Seeley et al. calculated the natural charge on chlorine in $ClONO_2$ to be +0.25 at the MP2/6-311+G(d) level.[36] Using the same level of theory, we calculated the natural charge on the Cl atom in $ClNO_2$ to be +0.06. Although the Cl atom is somewhat less electropositive in $ClNO_2$ than in $ClONO_2$, we propose that Cl^- + $ClNO_2$ proceeds via a similar mechanism to that of Cl^- + $ClONO_2$.

Seisel et al. proposed a mechanism for the heterogeneous reaction of N_2O_5 + HBr on ice that is similar to the mechanism that we propose for the reaction of HCl with HNO_3 solutions.[37] Using mass spectrometry techniques, Seisel et al. positively identified Br_2 and HONO as products from the reaction of N_2O_5 + HBr on ice, and presented some evidence for the existence of BrNO as a product, as well. However, no $BrNO_2$ was observed as a product. On the basis of their work on the heterogeneous reaction of N_2O_5 + HCl on ice, in which $ClNO_2$ was the predominant product observed, Seisel et al. proposed the following mechanism for N_2O_5 + HBr:

$$HBr + N_2O_5 \rightarrow BrNO_2 + HNO_3 \quad (38)$$

$$HBr + BrNO_2 \rightarrow Br_2 + HONO \quad (39)$$

$$HBr + HONO \rightarrow BrNO + H_2O \quad (40)$$

$$3HBr + N_2O_5 \rightarrow Br_2 + BrNO + HNO_3 + H_2O \quad (41)$$

This mechanism is very similar to the one that we propose for reaction 16. Seisel et al. speculate that for the reaction of N_2O_5 + HCl on ice, the $ClNO_2$ product produced in the first step of the mechanism is sufficiently stable such that it can be directly observed (while $BrNO_2$ was too reactive to be observed in their study of N_2O_5 + HBr). Seisel et al. further suggest that the key step in the mechanism is actually an ionic one:

$$Br^- + N_2O_5 \rightarrow [Br^- \cdots NO_2^+ \cdots NO_3^-] \rightarrow BrNO_2 + NO_3^- \quad (42)$$

If N_2O_5 is viewed as a complex of NO_2^+ and NO_3^-, as depicted above, this ionic reaction mechanism can be directly compared to the first step (reaction 23) in our ionic mechanism for reaction 16. We suggest that the N_2O_5 + HCl reaction on ice might proceed via a similar mechanism to the one that we propose for reaction 16. Therefore, it appears that a similar ionic mechanism is capable of rationalizing the oxidation of halides by nitrogen oxides of differing forms (HNO_3 and N_2O_5) and in differing media (acid solutions and ice).

Conclusions

Using a closed system reactor and chemical ionization mass spectrometry, UV−Vis, and IR spectroscopy detection methods, we determined that HCl can be converted into the species Cl_2, ClNO, and $ClNO_2$ via the reaction with $HNO_3/H_2SO_4/H_2O$ solutions. We proposed an overall reaction (3HCl + HNO_3 →

$Cl_2 + ClNO + 2H_2O$) and an ionic mechanism where NO_2^+ and Cl^- are the key reactive species. Our proposed ionic mechanism is very similar to proposed mechanisms for the reaction of HBr and HCl with N_2O_5 and the Cl_2-producing step of our mechanism is similar to mechanisms proposed for the heterogeneous reaction of HCl with $ClONO_2$. Temperature-dependent kinetic studies were carried out on acid solutions that model the composition of polar stratospheric aerosols in order to assess the role of this process in the activation of stratospheric chlorine. The HCl processing rate for this reaction was estimated at polar stratospheric conditions and shown to be minor in comparison to both the major gas phase and heterogeneous chlorine activation pathways.

Acknowledgment. This research was funded by grants from the National Science Foundation (ATM-9874752), Camille and Henry Dreyfus Foundation, American Chemical Society − Petroleum Research Fund, and Research Corporation. We thank Kurt Scholtens and Ben Messer for their assistance with the mass spectrometry experiments and Brad Mulder for his assistance with the temperature-dependent studies.

References and Notes

(1) Solomon, S.; Garcia, R. R.; Rowland, F. S.; Wuebbles, D. J. *Nature* **1986**, *321*, 755.

(2) Molina, M. J. In *The Chemistry of the Atmosphere: Its Impact on Global Change*; Calvert, J. G., Ed.; Blackwell Scientific: Boston, 1994.

(3) Molina, M. J.; Zhang, R.; Wooldrige, P. J.; McMahon, J. R.; Kim, J. E.; Chang, H. Y.; Beyer, K. D. *Science* **1993**, *261*, 1418.

(4) Schreiner, J.; Voigt, C.; Kohlmann, A.; Arnold, F.; Mauersberger, K.; Larsen, N. *Science* **1999**, *283*, 968.

(5) Kolb, C. E.; Worshop, D. R.; Zahauser, M. S.; Davidovits, P.; Keyser, L. F.; Leu, M. T.; Molina, M. J.; Hanson, D. R.; Ravishankara, A. R.; Williams, C. R.; Tolbert, M. A. In *Progress and Problems in Atmospheric Chemistry*; World Scientific: Singapore, 1995.

(6) Jaegle, L.; Webster, C. R.; May, R. D.; Scott, D. C.; Stimpfle, R. M.; Kohn, D. W.; Wennberg, P. O.; Hanisco, T. F.; Cohen, R. C.; Proffitt, M. H.; Kelley, K. K.; Elkins, J.; Baumgardner, D.; Dye, J. E.; Wilson, J. C.; Pueschel, R. F.; Chan, K. R.; Salawitch, R. J.; Tuck, A. F.; Hovde, S. J.; Yung, Y. L. *J. Geophys. Res.* **1997**, *102*, 13235.

(7) See for example, *Faraday Discuss.* **1995**, *100*, 333.

(8) Bostwick, L. E. *Chem. Eng.* **1976**, 86.

(9) Schreiner, W. C.; Cover, A. E.; Hunter, W. D.; van Dijk, C. P.; Jongenburger, H. S. *Hydrocarb. Process.* **1974**, 151.

(10) Van Dijk, C. P.; Schreiner, W. C. *Chem. Eng. Prog.* **1973**, *69*, 57.

(11) Johnstone, H. F. *Chem. Eng. Prog.* **1948**, *44*, 657.

(12) Luick, T. J.; Heckert, R. W.; Schulz, K.; Disselkamp, R. S. *J. Atmos. Chem.* **1999**, *32*, 315.

(13) Massucci, M.; Clegg, S. L.; Brimblecombe, P. *J. Phys. Chem. A* **1999**, *103*, 4209.

(14) Longfellow, C. A.; Imamura, T.; Ravishankara, A. R.; Hanson, D. R. *J. Phys. Chem. A* **1998**, *102*, 3323.

(15) Scholtens, K. W.; Messer, B. M.; Cappa, C. D.; Elrod, M. J. *J. Phys. Chem. A* **1999**, *103*, 4378.

(16) Huey, L. G.; Hanson, D. R.; Howard, C. J. *J. Phys. Chem.* **1995**, *99*, 5001.

(17) Streit, G. E. *J. Chem. Phys.* **1982**, *77*, 826.

(18) Nakamoto, K. *Infrared Spectra of Inorganic and Coordination Compounds*; John Wiley & Sons: New York, 1963; Part II.

(19) Mellor, J. W. *A Comprehensive Treatise on Inorganic and Theoretical Chemistry*; Longmans, Green and Co.: London, 1928; Vol. VIII, pp 612−624.

(20) Burley, J. D.; Johnston, H. S. *Geophys. Res. Lett.* **1992**, *19*, 1359.

(21) MacTaylor, R. S.; Gilligan, J. J.; Moody, D. J.; Castleman, A. W., Jr. *J. Phys. Chem. A* **1999**, *103*, 4196.

(22) Banham, S. F.; Horn, A. B.; Koch, T. G.; Sodeau, J. R. *Faraday Discuss.* **1995**, *100*, 321.

(23) Burley, J. D.; Johnston, H. S. *Geophys. Res. Lett.* **1992**, *19*, 1363.

(24) Zhang, R.; Leu, M. T.; Keyser, L. F. *J. Phys. Chem.* **1996**, *100*, 339.

(25) Fenter, F. F.; Rossi, M. J. *J. Phys. Chem.* **1996**, *100*, 13765.

(26) Carslaw, K. S.; Clegg, S. L.; Brimblecombe, P. *J. Phys. Chem.* **1995**, *99*, 11557.

(27) Tabazadeh, A.; Turco, R. P.; Jacobson, M. Z. *J. Geophys. Res.* **1994**, *99*, 12897.

(28) Del Negro, L. A.; Fahey, D. W.; Donnelly, S. G.; Gao, R. S.; Keim, E. R.; Wamsley, R. C.; Woodbridge, E. L.; Dye, J. E.; Baumgardner, D.; Gandrud, B. W.; Wilson, J. C.; Jonsson, H. H.; Loewenstein, M.; Podolske, J. R.; Webster, C. R.; May, R. D.; Worsnop, D. R.; Tabazadeh, A.; Tolbert, M. A.; Kelly, K. K.; Chan, K. R. *J. Geophys. Res.* **1997**, *102*, 13255.

(29) Hanson, D. R. *J. Phys. Chem. A* **1998**, *102*, 4794.

(30) Borrman, S.; Solomon, S.; Dye, J. E.; Baumgardner, D.; Kelly, K. K.; Chan, K. R. *J. Geophys. Res.* **1997**, *102*, 3639.

(31) Battin-Leclerc, F.; Kim, I. K.; Talukdar, R. K.; Portmann, R. W.; Ravishankara, A. R.; Steckler, R.; Brown, D. *J. Phys. Chem. A* **1999**, *103*, 3237.

(32) DeMore, W. B.; Sander, S. P.; Howard, C. J.; Ravishankara, A. R.; Golden, D. M.; Kolb, C. E.; Hampson, R. F.; Kurylo, M. J.; Molina, M. J. *Chemical Kinetics and Photochemical Data for Use in Stratospheric Modeling*; JPL Publication 97-4; Jet Propulsion Laboratory: Pasadena, CA, 1997.

(33) Bianco, R.; Hynes, J. T. *J. Phys. Chem. A* **1999**, *103*, 3797.

(34) Horn, A. B.; Sodeau, J. R.; Roddis, T. B.; Williams, N. A. *J. Phys. Chem. A* **1998**, *102*, 6107.

(35) Frisch, M. J.; Trucks, G. W.; Schlegel, H. B.; Gill, P. M. W.; Johnson, B. G.; Robb, M. A.; Cheeseman, J. R.; Keith, T. A.; Petersson, G. A.; Montgomery, J. A.; Raghavachari, K.; Al-Laham, M. A.; Zakrzewski, V. G.; Oritz, J. V.; Foresman, J. B.; Cioslowski, J.; Stefanov, B. B.; Nanayakkara, A.; Challacombe, M.; Peng, C. Y.; Ayala, P. Y.; Chen, W.; Wong, M. W.; Andres, J. L.; Replogle, E. S.; Gomperts, R.; Martin, R. L.; Fox, D. J.; Binkley, J. S.; DeFrees, D. J.; Baker, J.; Stewart, J. P.; Head-Gordon, M.; Gonzalez, C.; Pople, J. A. *GAUSSIAN 94*, *Revision E.2*; Gaussian: Pittsburgh, PA, 1995.

(36) Seeley, J. V.; Miller, T. M.; Viggiano, A. A. *J. Chem. Phys.* **1996**, *105*, 2127.

(37) Seisel, S.; Flückiger, B.; Rossi, M. J. *Ber. Bunsen. Phys. Chem.* **1998**, *102*, 811.